Liquid-Crystalline Polyimides. 12. Fully Aromatic Thermotropic Poly(Ester-imide)s Derived from Diphenylether-3,3',4,4'-Tetracarboxylic Imide

Hans R. Kricheldorf[a]; Volker Linzer[a]; Javier De abajo[b]; José De la campa[b]

[a] Institut für Technische und Makromolekulare Chemie Universität Hamburg Bundesstrasse 45, Hamburg, Germany [b] Instituto de la Ciencia y Tecnologia de Polimeros Calle Juan de la Cierva 3, Madrid, Spain

PLEASE SCROLL DOWN FOR ARTICLE

LIQUID-CRYSTALLINE POLYIMIDES. 12. FULLY AROMATIC THERMOTROPIC POLY(ESTER-IMIDE)S DERIVED FROM DIPHENYLETHER-3,3′,4,4′-TETRACARBOXYLIC IMIDE

HANS R. KRICHELDORF* and VOLKER LINZER

Institut für Technische und Makromolekulare Chemie
Universität Hamburg
Bundesstrasse 45, D-20146 Hamburg, Germany

JAVIER DE ABAJO and JOSÉ DE LA CAMPA

Instituto de la Ciencia y Tecnologia de Polimeros
Calle Juan de la Cierva 3, 28006 Madrid, Spain

ABSTRACT

Acetylated imide diphenols were prepared from 3- or 4-aminophenol and diphenylether-3,3′,4,4′-tetracarboxylic anhydride, benzophenone-3,3′,4,4′-tetracarboxylic anhydride, diphenylsulfone-3,3′,4,4′-tetracarboxylic anhydride, or hexafluoroisopropylidene diphenyl-3,3′,4,4′-tetracarboxylic anhydride. These acetylated imide diphenols were polycondensed with substituted terephthalic acids or naphthalene-2,6-dicarboxylic acid. All poly(ester-imide)s, PEIs, derived from 3-aminophenol exclusively formed isotropic melts. A thermotropic character was found for PEIs based on 4-aminophenol and diphenylether-3,3′,4,4′-tetracarboxylic acid. In contrast, the diphenylsulfone and isopropylidene diphenyl building blocks proved to be unfavorable for the formation of liquid-crystalline phases. Energy minima, bond angles, and torsion angles of the imide units were calculated by a force-field program, and the experimental results are discussed on the basis of these theoretical data. Furthermore, three different force-field programs are compared.

311

INTRODUCTION

Amorphous, isotropic poly(ester-imide)s are commercially used as insulating lacquers for electric wires, whereas thermotropic, aromatic poly(ester-imide)s [1–7] are of interest as high performance engineering plastics or fibers. In the preceding part [1] of this series, poly(ester-imide)s derived from monomers **1a** and **1b** were studied. The formation of a nematic melt was only observed for polymers prepared from the 4-aminophenol derivative **1b**, whereas the 3-aminophenol derivative yielded isotropic materials. Unfortunately, the melting temperatures (T_m) of the LC-poly(ester-imide)s derived from **1b** were too high for convenient processing. In order to obtain structure–property relationships on a broader basis and LC-poly(ester-imide)s with lower melting points, the present work had the purpose of studying poly(ester-imide)s based on 3- or 4-aminophenol and four different tetracarboxylic dianhydrides.
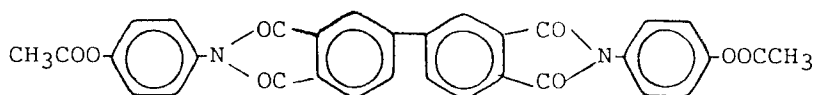
<u>1a</u>: meta substitution
<u>1b</u>: para substitution

EXPERIMENTAL

Materials

3- and 4-Aminophenol and benzophenone-3,3′,4,4′-tetracarboxylic anhydrides were gifts of Bayer AG (Leverkusen). They were used without further purification. Diphenylsulfone-3,3′,4,4′-tetracarboxylic anhydride and diphenylether-3,3′,4,4′-tetracarboxylic anhydride were gifts of Amoco Co. (Naperville, Illinois, USA); 2,2-diphenyl hexafluoropropane tetracarboxylic anhydride was a gift of Hoechst AG (Hoechst, Germany). All these anhydrides were recrystallized from dioxane/acetic anhydride. Naphthalene-2,6-dicarboxylic acid was a gift of Amoco Co. and used without further purification. The substituted terephthalic acids and their trimethylsilylesters were described in previous papers [1, 8–10].

Synthesis of Acetylated Imide Diphenols [2–4]

A tetracarboxylic anhydride (0.15 mol) was dissolved in dry dimethylformamide, and 4-aminophenol (0.31 mol) was added portionwise. The resulting solution was heated to 80°C for 2 hours and then acetic anhydride (0.5 mol) was added. The reaction mixture was heated to 120°C for 2 hours, cooled, and precipitated into cold water. The precipitated product was isolated by filtration, washed with cold water, and recrystallized from a mixture of 1,4-dioxane and a small amount of water.

Silylation of Dicarboxylic Acids

A dicarboxylic acid (0.4 mol) and hexamethyl disilazane (0.5 mol) were refluxed in dry toluene until the evolution of NH_3 ceased. The reaction mixture was then concentrated in vacuo, and the product was isolated by distillation over a short-path apparatus in the best possible vacuum at bath temperatures in the 140 to 240°C range.
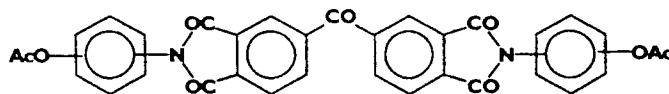
Polycondensations

With Free Dicarboxylic Acids

An acetylated imide diphenol (**2a**, **2b**, **3a**, **3b**, **4**, or **5**) (30 mmol), a dicar-
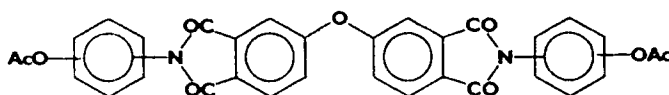
2a : meta
3b : para

3a : meta
3b : para
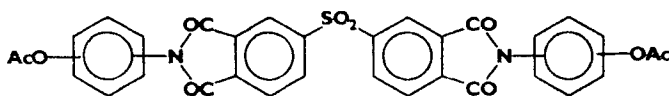
4
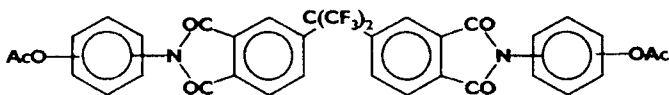
5

boxylic acid (30 mmol), and magnesium oxide (5-10 mg) were weighed into a cylindrical glass-reactor equipped with stirrer, gas-inlet, and gas-outlet tubes. The reactor was placed into a metal bath preheated to 150°C, and the temperature was rapidly raised to 260°C where the polycondensation slowly started. The temperature was further raised in 10°C steps to 320°C over a period of 3 hours. Finally, vacuum was applied for 0.5 hour.

With Silylated Dicarboxylic Acids

An acetylated diphenol (10 mmol), a silylated dicarboxylic acid (10 mmol), and titanium tetraisopropoxide (0.01 mmol in toluene) were weighed under nitrogen into a cylindrical glass-reactor. The reaction vessel was placed into a metal bath and heated to 300°C to obtain a homogeneous melt. The temperature was then lowered to 260–270°C so that smooth polycondensation took place. The temperature was then raised to 320°C over a period of 4 hours, and vacuum was applied for 0.5 hour. The cold product was ground and extracted with hot acetone, or in the case of **8a** dissolved in CH_2Cl_2/trifluoroacetic acid, and precipitated into methanol.

Measurements

Inherent viscosities, WAXS powder patterns, and DSC curves were measured as described previously [1, 4–7]. The IR spectra were recorded with a Nicolet SXB-20 FT-IR spectrometer from KBr pellets.

Computational Methods

The force-field energy minimization and molecular dynamic simulations were carried out on an IBM RS/6000 workstation. The simulations were carried out by employing the consistent valence force field (CVFF) and its PCFF91 version as incorporated in Insight II V2.2.0/Discover V2.8.0 molecular modeling software package developed by Biosym Technology, San Diego, California, USA, June 1993.

RESULTS AND DISCUSSION

Syntheses

The acetylated imide diphenols **2a**, **2b**, **3a**, **3b**, **4**, and **5** were synthesized from free aminophenols and the corresponding dianhydrides by a "one-pot-procedure" also used for monomers **1a** and **1b** [1]. The yield and properties of these monomers are listed in Table 1. To the best of our knowledge, these monomers have not been described in the literature before. Therefore, they were characterized by elemental analyses and ^{1}H-NMR and IR spectroscopy. As illustrated in Fig. 1, all ^{1}H-NMR spectra display the singlet signal of the acetate group around 2.2 ppm. In the case of aminophenol derivatives, two doublet signals of the *para*-substituted phenylene rings show up between 7.1 and 7.5 ppm. The IR spectra (Fig. 2) exhibit the "ester CO band" around 1750 cm^{-1} and the two characteristic "imide CO bands" at 1700 and 1770 cm^{-1}.
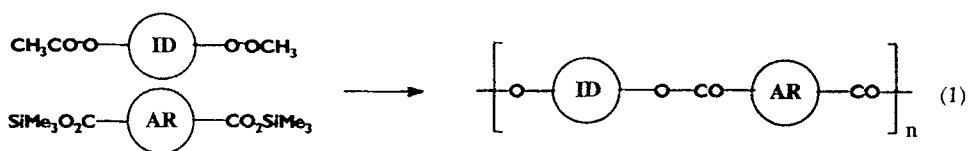
The monomers **2a**, **3a**, **4**, and **5** were polycondensed with free dicarboxylic acids in bulk (Method A) because homogeneous melts were obtained below 300°C at the beginning of the polycondensation. However, in the case of **2b** and **3b**, an initial reaction temperature ≥340°C is required, and at such high temperatures both the diphenol acetates and the dicarboxylic acids decompose. Therefore, a recently published [11, 12] new condensation program (Method B) was utilized.

TABLE 1.   Yields and Properties of Acetylated Imide Diphenols **2a**, **2b**, **3a**, **3b**, **4**, and **5**

Formula	Yield, %	mp, °C	Elemental formula (formula weight)		Elemental analyses		
					C	H	N
2a	47	205–206[a]	$C_{32}H_{20}N_2O_9$	Calcd.	66.67	3.50	4.86
			(576.5)	Found	66.50	3.42	4.90
2b	77	337[a]	$C_{32}H_{20}N_2O_9$	Calcd.	66.67	3.50	4.86
			(576.5)	Found	66.53	3.67	4.84
3a	30	264–266	$C_{33}H_2N_2O_9$	Calcd.	71.43	3.43	4.76
			(588.5)	Found	71.01	3.35	4.95
3b	41	375	$C_{33}H_2N_2O_9$	Calcd.	71.43	3.43	4.76
			(588.5)	Found	70.19	3.17	4.70
4	65	258–260	$C_{32}H_{20}N_2O_{10}S$	Calcd.	61.54	3.21	4.49
			(624.6)	Found	61.09	3.42	4.26
5	48	241–243	$C_{35}H_{20}F_6N_2O_8$	Calcd.	59.14	2.84	3.94
			(710.5)	Found	59.00	2.91	4.00

[a]After recrystallization.

This method is based on the condensation of a silylated carboxyl group with acetylated phenol groups (Eq. 1). This approach has three advantages. First, the melting points of the silylated dicarboxylic acids are relatively low (usually <200°C), and allow the formation of homogeneous reaction mixtures <300°C

$$CH_3COO-\text{(ID)}-OOCH_3$$
$$SiMe_3O_2C-\text{(AR)}-CO_2SiMe_3 \longrightarrow \left[O-\text{(ID)}-O-CO-\text{(AR)}-CO\right]_n \quad (1)$$

(ID) : unit of 2b or 3b

(AR) : bivalent aromatic residues (s. 7a-c and 8a,b)

even in the case of monomers **2b**. Second, the silylation prevents rapid decarboxylation. Third, the absence of acid protons reduces the risk of acid-catalyzed side reactions, such as the Fries rearrangement. Nonetheless, the high melting point of monomer **3b** prevents a successful polycondensation even with silylated dicarboxylic acids as reaction partners. The yields and properties of poly(ester-imide)s **6a–c**

6a-c

a: (AR) =   b: (AR) =

c: (AR) =

7a-c

a: (AR) =   b: (AR) =

c: (AR) =   d: (AR) =

e: (AR) =
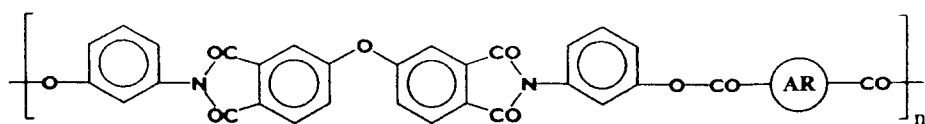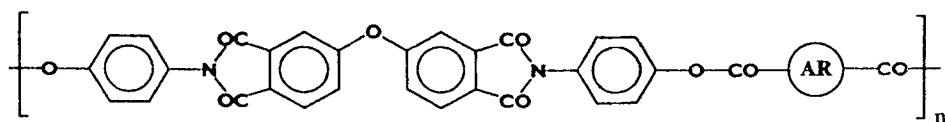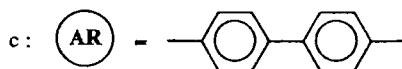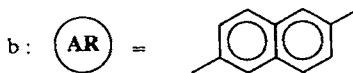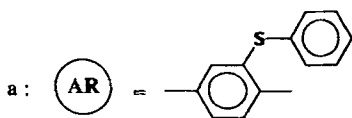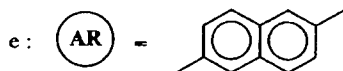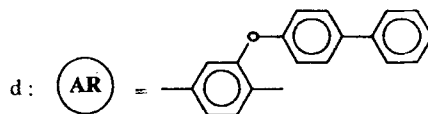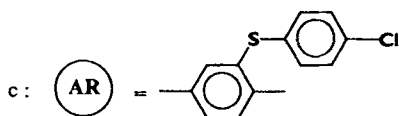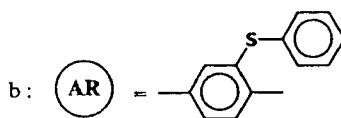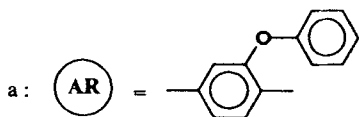
(prepared by Method A) and **7a–e** (Method B) are listed in Table 2. The yields and properties of poly(ester-imide)s **8a, 8b, 9a, 9b**, and **10** (prepared by Method A) are compiled in Table 3. The syntheses and properties of the silylated dicarboxylic acids required for Method B were reported in the preceding part [1].

8a-b

a : (AR) =   b : (AR) =

9a-b

a : (AR) =   b : (AR) =
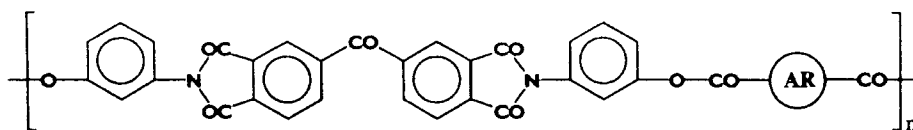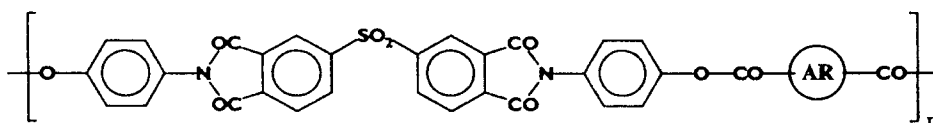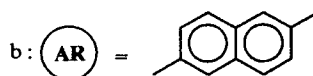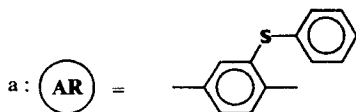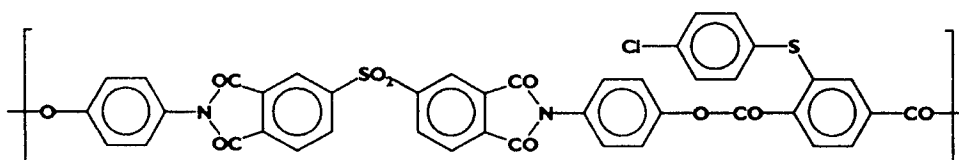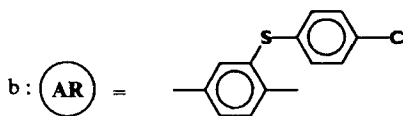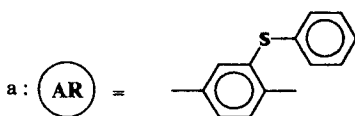
10

Characterization

As illustrated by Fig. 3, the IR spectra of all PEIs show a weak sharp "CO band" of the imide rings at 1770–1780 cm^{-1} and a broad intensive absorption between 1720 and 1750 cm^{-1} which represents the main CO band of the imide groups. This "imide band" overlaps with the "aromatic ester band" which absorbs 20–30 cm^{-1} lower than the aliphatic ester groups (Fig. 2). The ^{13}C-NMR spectra of **6a** and **9b** recorded in CHCl$_3$/trifluoroacetic acid exhibit two CO signals of the ester groups which are not identical due to asymmetry of the monosubstituted tereph- thalic acid. Furthermore, two CO signals of the imide groups are detectable.
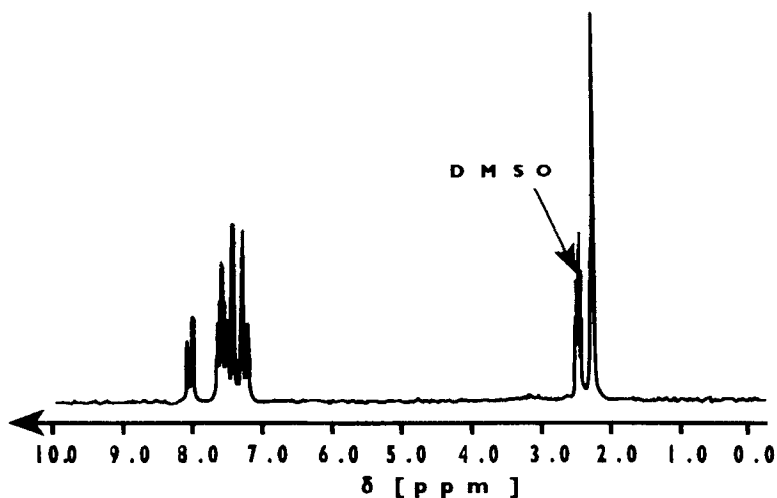
FIG. 1.   100 MHz ^{1}H-NMR spectrum of monomer **2b**.

All PEIs were further characterized by DSC measurements, WAXD powder patterns, and optical microscopy with crossed polarizers. It turned out that all PEIs based on 3-aminophenol as building block (**6a–c, 8a, 8b, 9a,** and **9b**) do not form a liquid-crystalline melt. This negative result agrees perfectly with the isotropic nature of the PEIs derived from **1a** [1]. With the exception of **8b,** all the aforementioned PEIs were found to be amorphous with glass-transition temperatures in the 180 to 230°C range (Tables 2 and 3). An amorphous and isotropic character was also revealed for PEI **10** despite the *para*-substitution of the phenylene rings. In the case
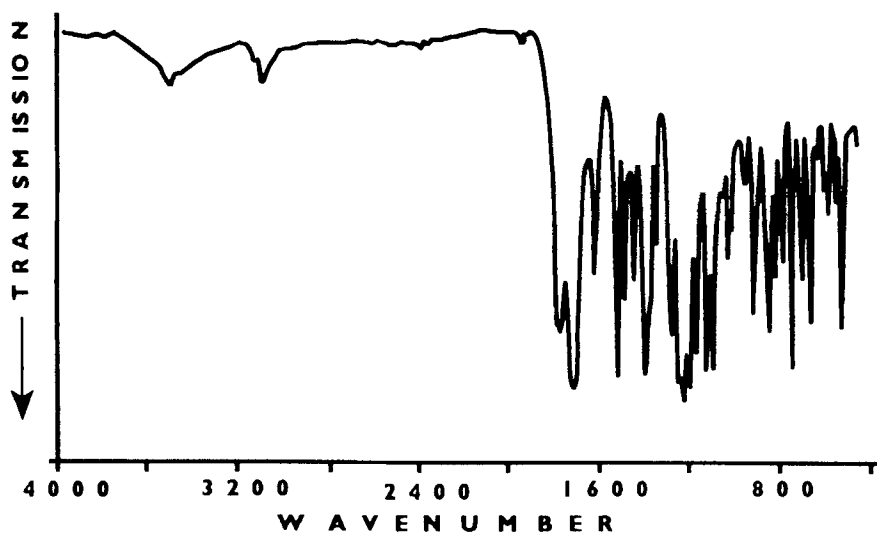
FIG. 2.   IR spectrum of monomer **2b** (KBr pellets).

TABLE 2. Yields and Properties of Poly(Ester-imide)s Derived from Diphenylether-3,3',4,4'-tetracarboxylic Anhydride and *meta*- or *para*-Aminophenol

Formula	T_{max}[a]	Yield, %	η_{inh},[b] dL/g	T_g,[c] °C	T_m,[c] °C	T_i,[d] °C	Elemental formula (formula weight)		Elemental analyses			
									C	H	N	S
6a	270	97	0.25	183	—	—	$C_{42}H_{22}N_2O_9S$ (730.7)	Calcd.	69.04	3.03	3.83	4.39
								Found	68.13	2.82	3.77	4.14
6b	270	90	0.32	215	—	—	$C_{40}H_{20}N_2O_2$ (672.6)	Calcd.	71.43	3.00	4.16	—
								Found	70.11	3.04	5.54	—
6c	300	38	0.25	205	—	—	$C_{42}H_{22}N_2O_9$ (698.65)	Calcd.	72.21	3.17	4.01	—
								Found	71.12	3.05	3.87	—
7a	300	87	—	195	376 (354)	380–385	$C_{42}H_{22}N_2O_{10}$ (714.6)	Calcd.	70.59	3.10	3.92	—
								Found	70.37	3.40	4.12	—
7b	300	85	—	206	370/390	410–415	$C_{42}H_{22}N_2O_9S$ (730.7)	Calcd.	69.04	3.03	3.83	4.39
								Found	68.80	3.15	3.82	4.15
7c	300	84	—	200	360 (378)	405–415	$C_{42}H_{21}ClN_2O_9S$ (765.12)	Calcd.	65.93	2.77	3.66	4.19
								Found	65.69	3.	3.72	4.05
7d	280	83	0.35	185	342	—	$C_{48}H_{20}N_2O_{10}$ (790.7)	Calcd.	72.91	3.31	3.54	—
								Found	71.09	3.07	3.57	—
7e	300	91	—	—	Crystalline, no melting detectable	—	$C_{40}H_{20}N_2O_9$ (672.6)	Calcd.	71.43	3.00	4.16	—
								Found	70.05	3.08	4.00	—

[a]Maximum reaction temperature at the end of polycondensation.
[b]Inherent viscosity measured at 20°C with $c = 2$ g/L in CH_2Cl_2/trifluoroacetic acid (volume ratio 4:1).
[c]From DSC measurements with a heating rate of 20°C/min (data from the second heating are in parentheses).
[d]From optical microscopy with crossed polarizers.

TABLE 3. Yields and Properties of Poly(Ester-imide)s **8a**, **9a**, **9b**, and **10** Derived from Various Diimide Diphenols

Formula	T_{max} [a]	Yield, %	η_{inh},[b] dL/g	T_g,[c] °C	T_m,[c] °C	Elemental formula (formula weight)		Elemental analyses			
								C	H	N	S
8a	300	95	0.28	182	—	$C_{43}H_{22}N_2O_9S$ (742.7)	Calcd.	69.54	2.99	3.77	4.32
							Found	68.67	3.28	3.69	3.99
8b	320	79	insol.	277	362	$C_{41}H_{20}N_2O_2$ (684.6)	Calcd.	71.93	2.94	4.09	—
							Found	70.65	3.12	4.15	—
9a	330	88	0.41	222	—	$C_{42}H_{22}N_2O_{10}S_2$ (778.7)	Calcd.	64.77	2.85	3.60	8.23
							Found	64.09	2.83	3.34	8.10
9b	330	94	0.38	228	—	$C_{42}H_{21}ClN_2O_{10}S_2$ (813.2)	Calcd.	61.99	2.60	3.45	7.89
							Found	61.90	2.52	3.34	7.81
10	320	95	0.25	205	—	$C_{45}H_{21}F_6ClN_2O_8S$ (899.2)	Calcd.	60.11	2.35	3.12	3.56
							Found	59.71	2.16	3.06	3.83

[a]Maximum reaction temperature at the end of polycondensation.
[b]Inherent viscosity measured at 20°C with c = 2 g/L in CH_2Cl_2/trifluoroacetic acid (volume ratio 4:1).
[c]From DSC measurements with a heating rate of 20°C/min (data from the second heating are in parentheses).
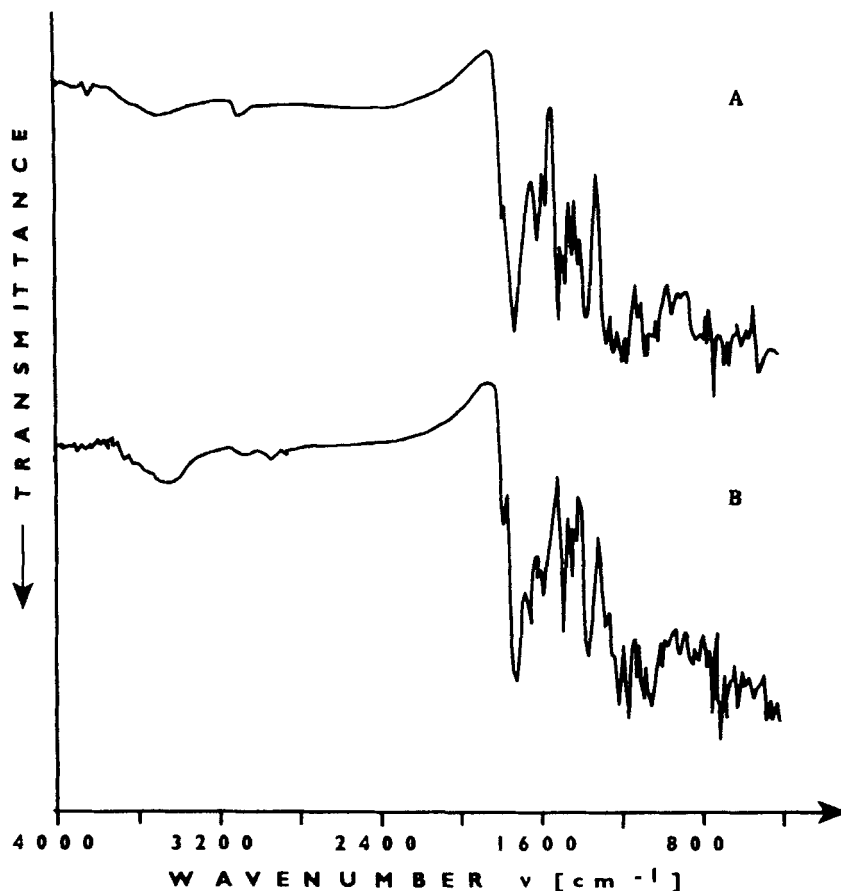[d]From optical microscopy with crossed polarizers.

FIG. 3.   IR spectra (KBr pellets) of (A) PEI **7b** and (B) PEI **8b**.

of poly(ester-imide) **8b**, the WAXS powder pattern of the "as-polymerized" sample revealed a low degree of crystallinity (Fig. 4). The DSC heating trace (Fig. 5) exhibits a glass-transition step at the unusually high temperature of 277°C. Furthermore, a strong melting endotherm was observable at 362°C with a shoulder at 385°C. However, no exotherm appeared in the cooling trace (measured at a rate of 20°C/min), suggesting that this polyester is a slowly crystallizing material. This suggestion was confirmed by both IR spectra and WAXD powder patterns. The IR spectrum recorded after heating to 390°C was identical with that measured before the heating (Fig. 3A). In other words, no significant thermal degradation had occurred. The WAXD powder pattern obtained after heating did not display the reflection present in Fig. 4. Only the "halo" of an entirely amorphous material was observed.

   The semicrystalline nature of PEIs **7a-e** was clearly evidenced by their WAXD powder patterns. As demonstrated by Figs. 6 and 7, the nature of the dicarboxylic acid has a tremendous influence on the structure of the WAXD patterns. In the case of **7a** the WAXD pattern suggests a tendency in the direction of orthorhombic chain
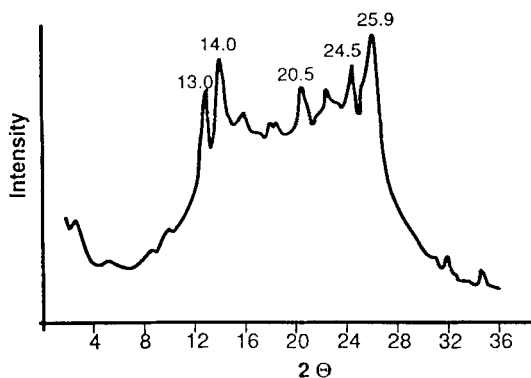
FIG. 4.   WAXD powder pattern of PEI **8b** (before heating).

packing whereas the powder pattern of **7e** is very similar to that of **8b** (Fig. 4), indicating the strong influence of 2,6-naphthoic acid on the structure of the crystal lattice.

The DSC measurements of **7e** and optical microscopy indicated that this poly-ester does not melt below 500°C. In contrast, all other members of this series showed a melting endotherm in the DSC heating trace below 400°C (Fig. 8). Optical microscopy revealed that in all four cases a nematic melt (Fig. 9) exists above the melting temperature (T_m). The temperature range of this nematic phase is relatively small due to thermal degradation above 400°C. Somewhat puzzling are the DSC traces of PEI **7b**. When heated to 450°C, three endotherms are detectable, but thermal degradation prevents any reproducibility. The third endotherm appears around 420–425°C and indicates the isotropization process. When the heating is stopped at 425°C (Fig. 8A), the cooling trace (Fig. 8B) shows the three correspond-ing exotherms. In agreement with optical microscopy, the high temperature exoth-erm (421°C) represents the anisotropization or, in other words, the formation of
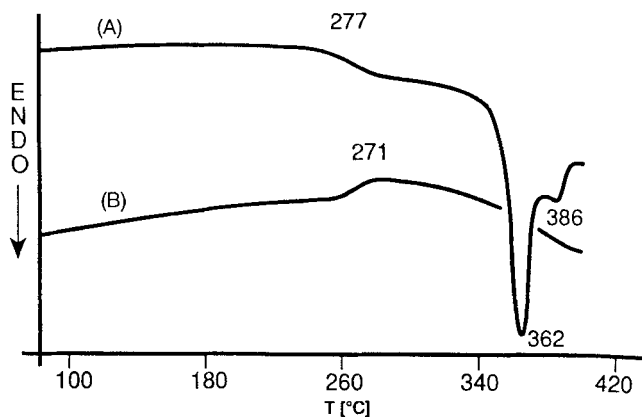

FIG. 5.   DSC measurements (heating/cooling rate, 20°C/min) of PEI **8b**: (A) first heating, (B) first cooling.
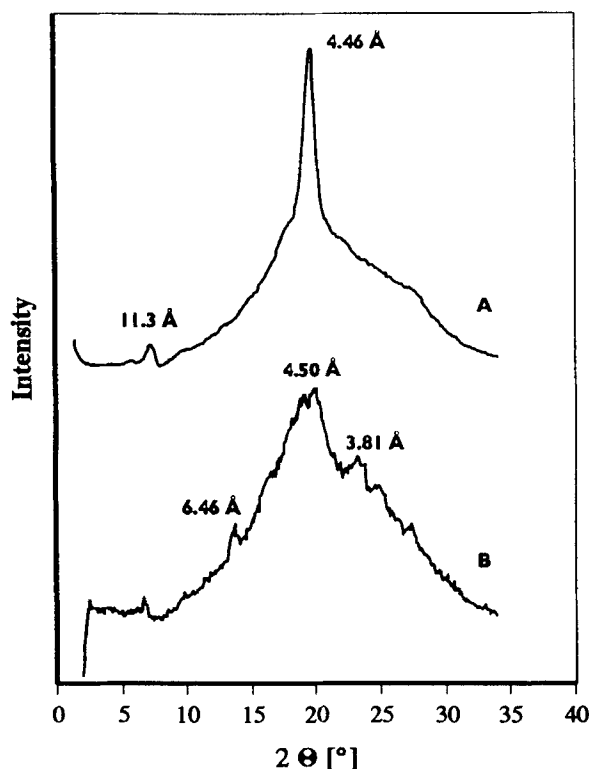
FIG. 6.   WAXD powder patterns of (A) PEI 7a and (B) PEI 7c.

the nematic phase. The endotherm at 390°C and the exotherm at 376°C indicate the melting and crystallization of PEI **7b**. Unclear is the role of the low temperature endotherm (369°C) and the exotherm at 273°C. An LC phase below the nematic phase should be a smectic phase. Yet the chemical structure of **7b** does not favor the formation of a layer structure because a regular sequence of polar and nonpolar segments is lacking. Furthermore, the WAXD pattern of **7b**, which is quite similar to that of **7a** (Fig. 6A), does not show any evidence of a layer structure. Another problem is the poor reproducibility of all phase transitions upon repeated heating and cooling. Thus, the meanings of the low temperature endotherm and exotherm remain unclear at this time.

Computer Modeling

The results of this work demonstrate that not only the polyester of monomer **1b** but also those of **2b** may be liquid-crystalline, despite the relatively unfavorable bond angle at the ether-oxygen and the flexibility of the ether group. On the other hand, polyester derived from monomer **5** was not liquid-crystalline. These results parallel the structure–property relationships found for aromatic polyesters of diphenols **11a-f** [13–15]. Whereas the polyesters derived from **11a-c** are liquid-crystalline, those of **11d-f** are not. Kricheldorf and Erxleben concluded [13] that the
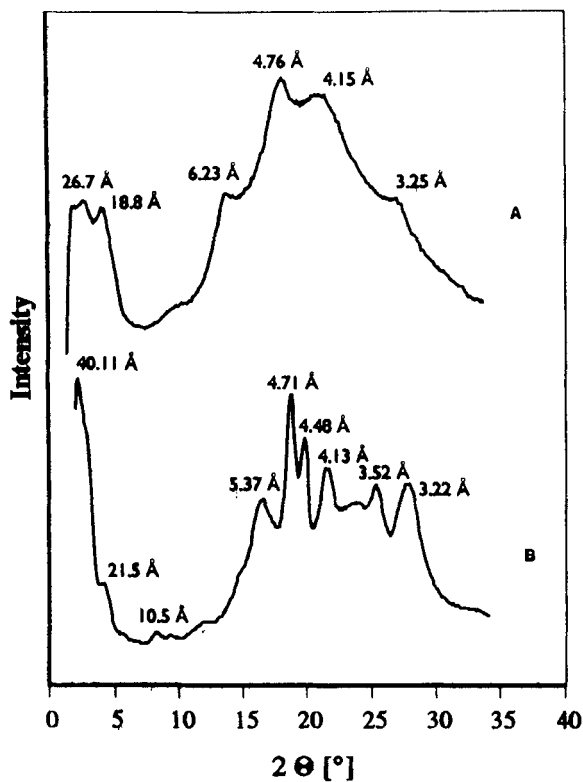
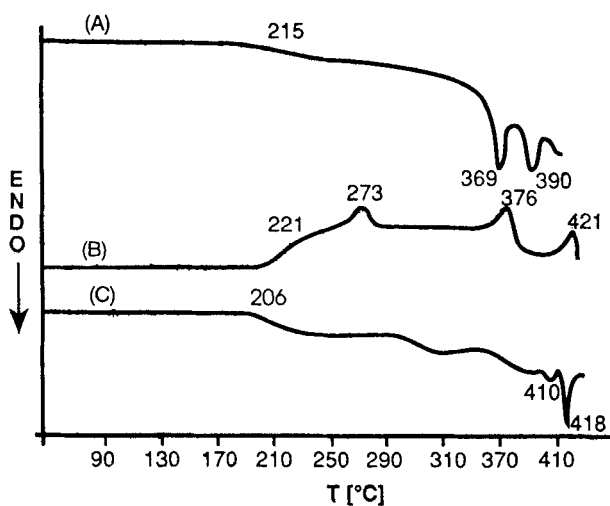FIG. 7.   WAXD powder patterns of (A) PEI **7d** and (B) PEI **7e**.

FIG. 8.   DSC measurements (heating/cooling rate, 20°C/min) of PEI **7b**: (A) first heating, (B) first cooling, (C) second heating.
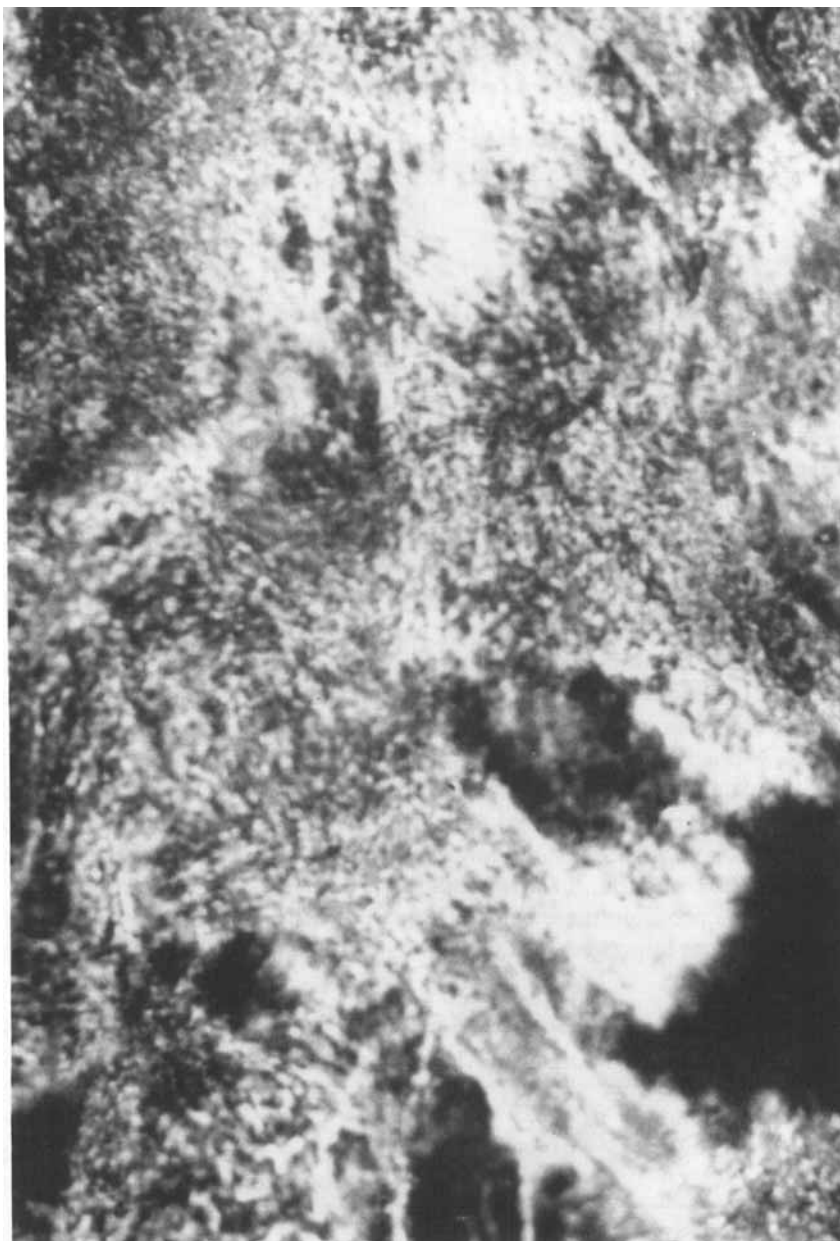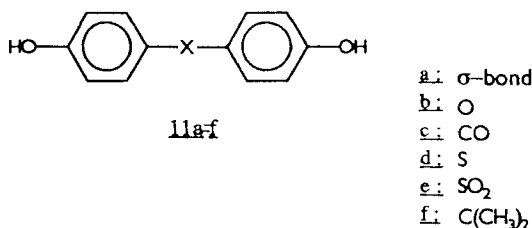
FIG. 9. Texture of PEI **7b** at 400°C.

11a-f

a: σ-bond
b: O
c: CO
d: S
e: SO₂
f: C(CH₃)₂

bond angle at the central X group (Table 4) plays a major role for mesogenic properties. Smaller bond angles are obviously unfavorable for calamitic (rodlike) mesogens. However, consideration of the bond angle alone is not satisfactory for the following reasons. The bond angles of diphenyl ether and benzophenone are 55–60° smaller than those of linear diphenyl derivatives, whereas the difference relative to diphenylsulfide or diphenylpropane derivatives is only on the order of 10–15°. In contrast, the properties of polyesters show a major difference between 4,4′-dihydroxydiphenylether and 4,4′-dihydroxybenzophenone, on the one hand, and bisphenol-A or 4,4′-dihydroxydiphenylsulfide, on the other hand. Quite analogously, the properties of the PEIs derived from **2b** resemble those derived from **1b**, but not those of polyester **10**. In order to get a better understanding of the mesogenic properties of nonlinear and nonsymmetrical building blocks, the results of computer modeling with one of the most advanced force-field programs available at this time were taken into account.

The *N*-phenylphthalimide unit was first studied by means of three different force-field programs (Fig. 10). In a recent publication, Orzeszko [16] concluded on the basis of the Tripos force-field (Alchemy II, Tripos Associates) programs that the imide nitrogen possesses bond angles typical of sp^3 hybridization. Furthermore, a rotation of 90° was found for the phenyl ring versus the imide group (Fig. 10A). Using the same program these calculations were confirmed by the present authors. However, with the improved consistent valence force field (CVFF) used in Biosym's

TABLE 4.   Bond Angles and Torsion Angles Calculated for Monomers 1–5 and Experimental Bond Angles of Model Compounds

Formula	Bond[a] angle, °C	Torsion[a] angle, °C	Model compound	Bond[b] angle, degrees
1b	180	51	Diphenyl	180
2b	119	37	Diphenylether	122/124
3b	123	22	4,4′-Dimethoxybenzophenone	121
4	105	85	4,4′-Diiododiphenylsulfone	106
5	109	45	Bisphenol-A	110
—	—	—	4,4′-Dimethyldiphenylsulfide	109

[a]Computer modeling with the PCFF91 force-field of Biosyms Discover V-2.8.0 program.

[b]Experimental data (mostly x-ray results) compiled in Ref. 10.

(A)
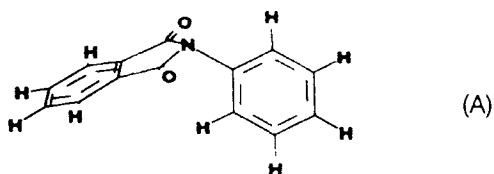
Minimized structure from Tripos-Forcefield
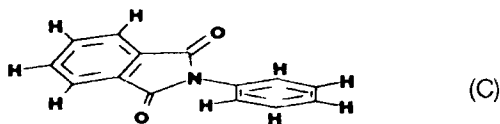(torsion angle 90°, bond angle 109°)

(B)
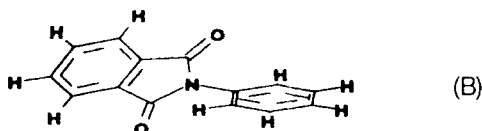
Minimized structure from CVFF-Forcefield *
(torsion angle 23°, bond angle 180°)

(C)

Minimized structure from PCFF91-Forcefield
(torsion angle 17°, bond angle 180°)

FIG. 10.   Minimum energy conformations of the *N*-phenylphthalimide group as calculated by three different force-field programs.

Discover V 2.8.0 Program, a bond angle of 180° and a rotational angle of 23° was obtained (Figure 10B). The latest development of the force-field method by Biosym Technology (PCFF91, June 1993) yielded a bond angle of 180° with a torsional angle of 17° (Fig. 10C). The results of these more advanced force-field programs are clearly in much better agreement with a mesogenic character of the *N*-phenylphthalimide units. The mesogenic character is evidenced by the fact that the PEIs of Structure 12 form a nematic melt which may be stable up to temperatures of 280°C in the case of short spacers [17].
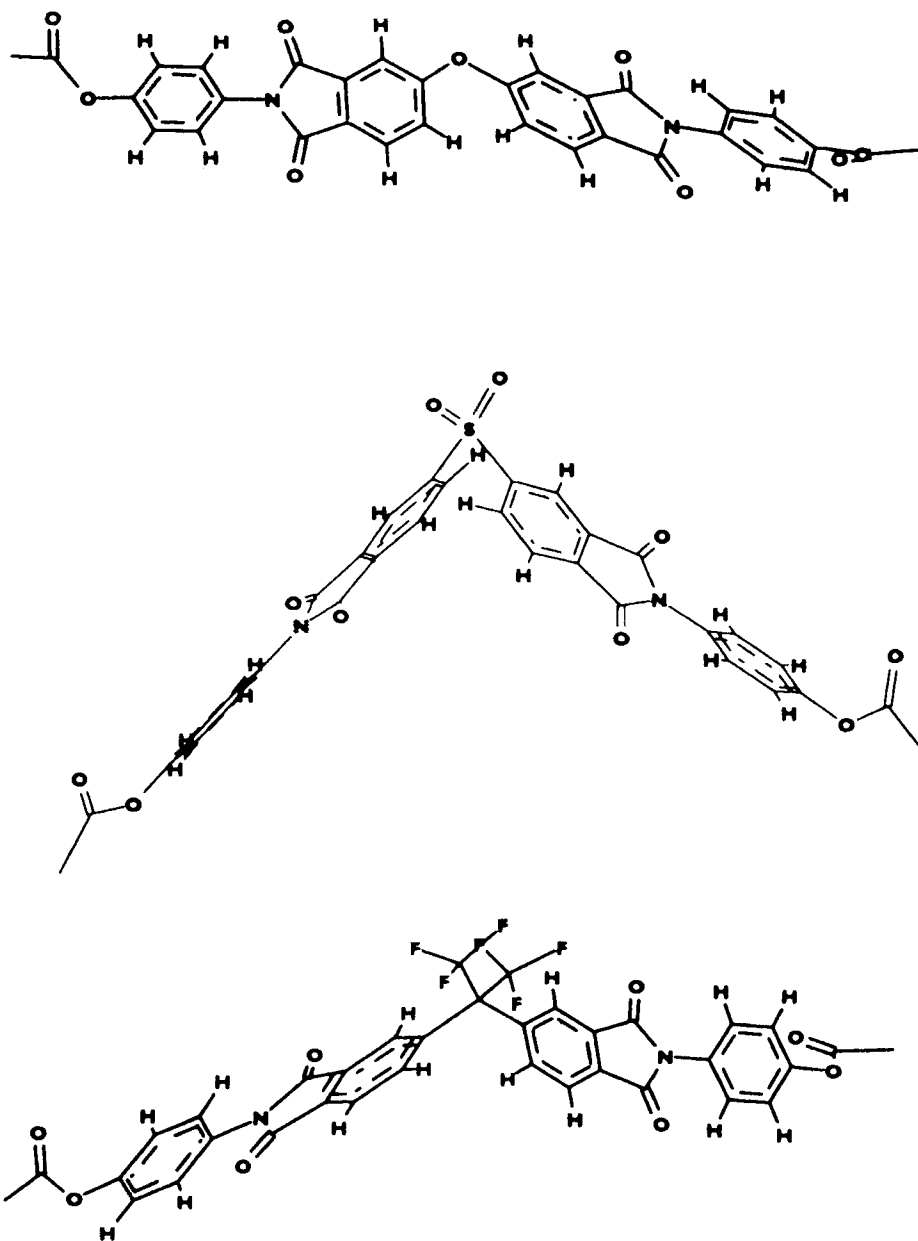

12
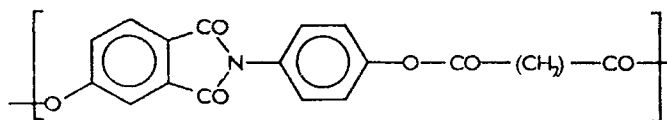
FIG. 11. Minimum energy conformations of three different repeating units as calculated by means of the PCFF91 force field used in Biosyms Discover V 2.8.0 Program.

Computer modeling of monomers 1-5 with the PCFF91 version of the Biosym Discover Program was conducted to elucidate the most stable conformation of the central part of the molecule. The bond angles and torsion angles obtained in this way are summarized in Table 4 along with the experimental data of some model compounds. Satisfactory agreement between calculated and experimental bond angle is evidenced with the exception of monomer 2b where the calculated angle is 3-5° smaller than that of diphenylether. Nonetheless, it is obvious that monomers 1-3 are more favorable as mesogens than monomers or repeating units based on diphenylsulfone or diphenylpropane derivatives such as 4 or 5.

Other interesting results are the low torsions angles of 2b and 3b relative to 4 and 5. The torsion angle is here defined as the rotation of one X-phthalimide axis out of the plane of the second phthalimide group. A small torsion angle indicates a tendency toward a coplanar system which is finally prevented by protons in the ortho position the X group. A high torsion angle means a "rooflike" conformation as illustrated by Fig. 11. Obviously the good mesogenic character of 2b and 3 or 11b and 11c has two reasons: the wider bond angles and the small torsion angles.

The role of wider bond angles is easy to understand because they favor a linear rodlike structure of the potential mesogen. However, the role of the torsion angles is difficult to rationalize on the basis of Onsager's [18] or Flory's [19, 20] definitions of rodlike mesogens. A planar conformation is advantageous when stacking of mesogenic groups with optimization of dipole–dipole and donor–acceptor interactions makes a significant contribution to the stabilization of the nematic order. As discussed more extensively in Part 15 of this series [21], the number of experimental results supporting this hypothesis is increasing. In this connection, not only are the torsion angles of the energy minimum conformation of interest but also the entire energy profiles of the rotation. Figure 12 illustrates that N-phenylphthalimide units, which are the basis of all imide mesogens reported so far, require only a
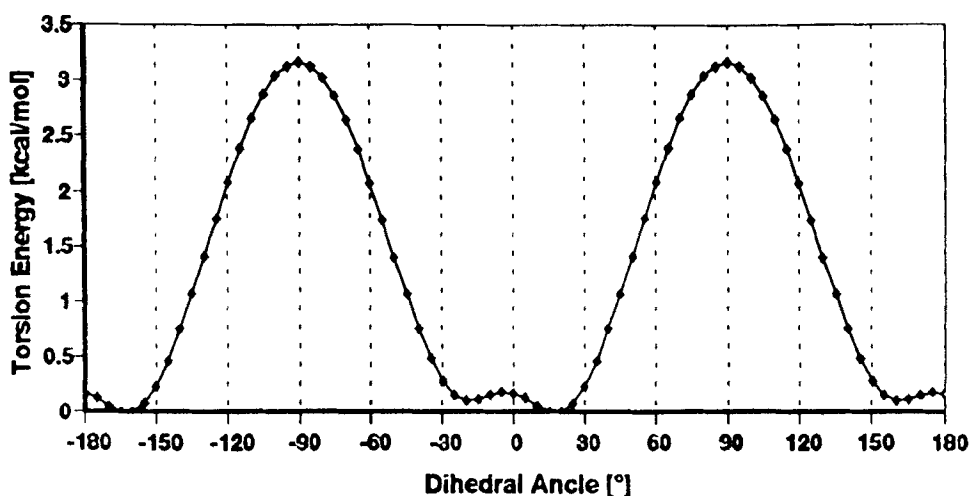

FIG. 12.   Energy profile of the rotation of N-phenylphthalimide in the configuration of Fig. 10(C) as calculated by PCFF91 used in the Biosyms Discover Program.

negligible amount of energy to adopt a planar conformation. Thus, this calculation supports the hypothesis that stacking and electronic interactions of mesogenic groups are important for the formation of LC phases of PEIs.

REFERENCES

[1]   H. R. Kricheldorf, V. Linzer, and C. Bruhn, *J. Macromol. Sci. — Pure Appl. Chem., A31*, 1315 (1994).

[2]   R. S. Irwin, US Patent 4,383,105 (1983), to E. I. DuPont Co.

[3]   W. Makoto, K. Fujiware, and H. Hideo, European Patent 314 173 (1989), to Idemitsu Petrochemical Corp.

[4]   H. R. Kricheldorf and R. Hüner, *Makromol. Chem., Rapid Commun., 11*, 211 (1990).

[5]   H. R. Kricheldorf, A. Domschke, and G. Schwarz, *Macromolecules, 24*, 1011 (1991).

[6]   J. de Abajo, J. G. de la Campa, H. R. Kricheldorf, and G. Schwarz, *Eur. Polym. J., 28*, 261 (1992).

[7]   H. R. Kricheldorf and R. Hüner, *J. Polym. Sci., Polym. Chem. Ed., 30*, 337 (1992).

[8]   H. R. Kricheldorf and V. Döring, *Makromol. Chem., 189*, 1425 (1988).

[9]   H. R. Kricheldorf and G. Schwarz, *Makromol. Chem., Rapid Commun., 10*, 243 (1989).

[10]   H. R. Kricheldorf and J. Engelhardt, *J. Polym. Sci., Polym. Chem. Ed., 28*, 2335 (1990).

[11]   H. R. Kricheldorf, G. Schwarz, and F. Ruhser, *Macromolecules, 24*, 3485 (1991).

[12]   H. R. Kricheldorf and D. Lübbers, *Makromol. Chem., Rapid Commun., 12*, 691 (1991).

[13]   H. R. Kricheldorf and J. Erxleben, *Polymer, 31*, 945 (1990).

[14]   R. W. Lenz and J.-I. Jin, *Macromolecules, 14*, 1405 (1981).

[15]   W. Zhang, J.-I. Jin, and R. W. Lenz, *Makromol. Chem., 189*, 2219 (1988).

[16]   E. Bialecka-Florjanczyk and A. Orzeszko, *Liq. Cryst., 15*(2), 255 (1993).

[17]   J. de Abajo, J. de la Campa, H. R. Kricheldorf, and G. Schwarz, *Makromol. Chem., 191*, 537 (1990).

[18]   L. A. Onsager, *Ann. N. Y. Acad. Sci., 51*, 627 (1949).

[19]   P. J. Flory, *R. Soc. London, A234*, 73 (1956).

[20]   P. J. Flory, *Adv. Polym. Sci., 59*, 1 (1984).

[21]   H. R. Kricheldorf, G. Schwarz, A. Domschke, and V. Linzer, *Macromolecules, 26*, 5161 (1993).